Agricultural and Forest Meteorology, 36 (1985) 19—28
Elsevier Science Publishers B.V., Amsterdam — Printed in The Netherlands

MODELING TRANSPIRATION PATTERNS OF VEGETATION ALONG SOUTH AND NORTH FACING SLOPES DURING THE SUBTROPICAL DRY SEASON

M. SEGAL[1], Y. MAHRER[2,3], R.A. PIELKE[1], and Y. OOKOUCHI [1,4]

[1] *Department of Atmospheric Science, Colorado State University, Fort Collins, CO 80523 (U.S.A.)*
[2] *Cooperative Institute for Research in the Atmosphere, Colorado State University, Fort Collins, CO 80523 (U.S.A)*
[3] *Permanent affiliation: Seagram Centre for Soil and Water Science, Faculty of Agriculture, The Hebrew University of Jerusalem, Rehovot 76100 (Israel)*
[4] *Permanent affiliation: Yatsushiro National College of Technology, Yatsushiro 866 (Japan)*

(Received August 8, 1984; revision accepted April 17, 1985)

ABSTRACT

Segal, M., Mahrer, Y., Pielke, R.A. and Ookouchi, Y., 1985. Modeling transpiration patterns of vegetation along south and north facing slopes during the subtropical dry season. Agric. For. Meterol., 36: 19—28.

The relationship between the inclination of south and north facing slopes, and the transpiration from vegetation is evaluated using numerical models for the dry season of the subtropical region of Israel. The accumulated transpiration for the dry season from canopies along south facing slopes was found to be maximized with a slope of about 22.5°. On north facing slopes, transpiration decreased monotonically with increasing slope angle. The relationship between the incoming solar radiation on the slopes and the resultant transpiration patterns is evaluated.

INTRODUCTION

Two well-recognized characteristics of relevance to the present study are: (i) The intensity of incoming solar radiation reaching inclined surfaces depends on the slope and azimuth of the terrain and (ii) the magnitude of the incoming solar radiation exerts an important role on transpiration from vegetation. Numerous studies have evaluated these aspects separately. To the best of our knowledge, however, the influence of various orientations of sloped terrain on the transpiration from vegetation has not been evaluated. A specific example of this terrain influence is evaluated in this paper by applying one-dimensional numerical models.

In the eastern Mediterranean area (as well as in other similar subtropical latitudes) the winter precipitation period is followed by a relatively long dry season in which the intensity of the solar radiation is extremely high. Mid-March is the beginning of the growing season in this region. Following this date precipitation is reduced considerably, and generally terminates several weeks later, not to commence again until around mid-November. Therefore,

0168-1923/85/$03.30

irrigation needs for agricultural activity in these geographic regions are substantial. In addition, the growth of natural shrubs and forests is limited because of the long summer drought. In mountainous areas of such regions, north facing slopes may be covered with natural vegetative cover such as shrubs, while the adjacent south facing slopes are bare or covered by less developed vegetation (e.g. Whittaker and Niering, 1965; Armesto and Martinez, 1978).

The purpose of the present study was to model vegetation transpiration patterns during the dry season in a typical subtropical region for south and north facing slopes. Israel (latitude 32°N) was chosen for this study. The azimuth orientation for these slopes provides the extreme cases for transpiration, whereas west and east facing slopes should reflect intermediate cases. We did not include evaluations for the last two slope orientations because of the generally asymmetric patterns of flow and precipitation along west—east cross sections of mountains in this region (e.g. Atlas of Israel, 1970). It is assumed that, in general, water needs are the prime factor determining vegetation growth in this season (factors such as soil type or soil nutrients, of course, are also of substantial importance). The interpretation of the transpiration patterns is directed toward indications of (i) the differences in the development of natural vegetation cover along these slopes, and (ii) the differences in irrigation needs involved with both slopes while considering agricultural activity.

MODELS ASPECTS

The atmospheric model

The atmospheric model adopted for the current study is described comprehensively in Pielke and Mahrer (1975) and Mahrer and Pielke (1977). Therefore, only a general outline is provided in the present paper.

The prediction equations for wind velocity, $\vec{V}$, the potential temperature, θ_p, and moisture, q, are

$$\frac{\partial \vec{V}}{\partial t} = -\vec{k}xf(\vec{V} - \vec{V}_g) + \frac{\partial}{\partial z}\left(K_M \frac{\partial V}{\partial z}\right) \tag{1}$$

$$\frac{\partial \theta_p}{\partial t} = \frac{\partial}{\partial z}\left(K_H \frac{\partial \theta_p}{\partial z}\right) + R \tag{2}$$

$$\frac{\partial q}{\partial t} = \frac{\partial}{\partial z}\left(K_Q \frac{\partial q}{\partial z}\right) \tag{3}$$

Where $\vec{V}_g$ is the geostrophic wind, f is the Coriolis parameter, and R is the radiation heating/cooling term. K_M, K_H, and K_Q are the eddy diffusion coefficients for momentum, heat, and specific humidity, respectively.

Parameterizations within the atmospheric model include calculations of the surface fluxes of momentum, heat and moisture according to Businger et

al. (1971). The eddy diffusion coefficients in the planetary boundary layer above the surface layer are of the O'Brien (1970) functional form. A prognostic equation is solved to predict the height of the planetary boundary layer. The temperature at the air—soil and air—vegetation interfaces are calculated using a heat balance equation which includes incoming longwave and solar radiation; latent, sensible, and soil heat fluxes; and the outgoing surface longwave radiation. The changes of air temperature, due to shortwave and longwave radiative flux divergence, are parameterized following the methods of Atwater and Brown (1974) and Sasamori (1972). Heating of the atmosphere by shortwave radiation is confined to absorption by water vapor, while carbon dioxide and water vapor are both considered in the longwave radiation heating—cooling algorithm.

The soil model

The following one-dimensional prediction equations for heat and moisture in the soil are used

$$\frac{\partial T_s}{\partial t} = \frac{1}{C_s}\frac{\partial}{\partial z}\left(\lambda_s \frac{\partial T_s}{\partial z}\right) \tag{4}$$

$$\frac{\partial \theta}{\partial t} = \frac{\partial}{\partial z}\left(D_\theta \frac{\partial \theta}{\partial z}\right) + \frac{\partial}{\partial z}\left(D_T \frac{\partial T_s}{\partial z}\right) + \frac{\partial K_h}{\partial z} - V_e(z, t) \tag{5}$$

where T_s is the soil temperature, t is time, z is depth, C_s is the soil volumetric heat capacity, λ_s is the soil thermal conductivity, θ is the soil volumetric wetness, D_θ is the soil moisture diffusivity, D_T is the soil moisture thermal diffusivity and K_h is the hydraulic conductivity. We assume that the soil medium is homogeneous and neglect the effect of hysteresis. C_s and λ are evaluated according to De Vries (1963) using the appropriate soil texture. D_θ and D_T are calculated using the matric potential according to Philip and De Vries (1957). $V_e(z, t)$ is the root water extraction term when vegetation exists. An empirical power curve formula based on a generalization of Kozeney and Carman's approach (Wyllie and Gardner, 1958) was used to calculated the soil hydraulic conductivity

$$K_h = K_{hs}\left(\frac{\theta - \theta_r}{\theta_s - \theta_r}\right)^n \tag{6}$$

where θ, θ_r and θ_s are the actual, saturation, and residual water contents, respectively, and K_{hs} is the hydraulic conductivity at saturation.

The matric potential was calculated from

$$\psi = \psi_{cr}\left(\frac{\theta - \theta_r}{\theta_s - \theta_r}\right)^{-\lambda} \tag{7}$$

where ψ_{cr} is the matric potential, obtained when the water content becomes

lower than the saturation water content in the $\psi(\theta)$ curve. When vegetation exists, the root extraction term $V_e(z, t)$, is assumed to be equal to the plant transpiration. Equations 4 and 5 are solved numerically using an implicit difference scheme as discussed in Paegle et al. (1976).

The initial conditions are obtained from profiles of soil temperature and moisture in a bare soil.

At the lower boundary of the soil T_s = constant and $\partial\theta/\partial z = 0$.

The vegetation model

The vegetation model formulation is based on that given in Avissar and Mahrer (1982) and Avissar et al. (1985). The vegetation is assumed to consist of a single layer in which temperature is computed from the energy budget equation

$$a_V R_{SV} + e_V R_{LV} - 2R_V - 2H_V - E_V = 0 \tag{8}$$

where R_{SV} and R_{LV} are the total short and longwave radiation respectively received at the vegetation surface, R_V is the radiation emitted by the vegetation, H_V and E_V are the sensible and latent heat fluxes between the vegetation and the surrounding air, a_V and e_V are the albedo and the emissivity of the vegetation, respectively. In order to solve the unknown representative temperature of the vegetation layer, a shading factor is defined as the ratio between the plant shadow on the ground and the total ground areas. This ratio is 1 for completely covered surface and 0 for bare soil. The net leaf area index, which is the ratio of total one-sided leaf area to the ground area covered by the vegetation, as well as the shading factor are needed to evaluate the different energy fluxes on the vegetation.

The vapor flux (transpiration), E, between a leaf and the ambient air temperature is expressed by the equation

$$E = ak^*(e_l^* - e_a) \tag{9}$$

whereas a is the coefficient for converting water vapor pressure to absolute humidity, $k^* = (h\ d_{rs}$ is the leaf—air transfer coefficient of latent heat, h is the potential leaf—air transfer coefficient of latent heat, d_{rs} is the relative stomatal conductance, e_l^* is the saturated vapor pressure of water of the leaf and e_a is the vapor pressure of ambient air. The expression for d_{rs} is given by

$$d_{rs} = [d_m + (d_M - d_m) F_R F_T F_V F_\psi F_c]/d_M \tag{10}$$

where d_m is the minimal conductance of the leaf cuticle when the stomata are closed, and d_M is the maximal stomatal conductance obtained when the stomata are completely open. Each of the F functions refers to the influence of a specific environmental factor upon the conductance (i.e., R for global solar radiation, T for leaf temperature, V for vapor pressure difference, C for ambient air CO_2 concentration and ψ for soil water potential). The range of values for F is 0—1 (when environmental factors completely close the

stomatal aperture, $F = 0$; when such factors are completely supportive, $F = 1$).

SIMULATION ASPECTS

Establishment of pertinent meteorological data set

The investigation period is from mid-March to mid-November. A data set with a fine time resolution (i.e., corresponding to the vegetation model time step) of wind speed, air temperature and moisture at a single elevation above the surface and solar radiation data are needed for this period in order to provide the needed input for the soil—vegetation model. Such meteorological data can be obtained at a specific site by measurements. However, since our study is oriented toward a general scaling of the influence of slope on the transpiration patterns of vegetation, the atmospheric model is used to obtain the surface meteorological characteristics. The monthly averaged profiles of temperature and moisture at Beer Ya'aqov, Israel (Shaia, 1962) were used for the initialization of the atmospheric model as well as for the daily forcing of the changes in the observed vertical tropospheric profiles of temperature and moisture during the period of study. The soil model was initialized with the Bet-Dagan mid-March temperature profile based on Zemel and Lomas (1977).

The large-scale wind speed was assumed to be $5\,\mathrm{m\,s^{-1}}$ at the top of the atmospheric planetary boundary layer with its daily variation within the surface layer predicted by similarly theory (see Mahrer and Pielke, 1977 for the adopted formulation). The time step of integration was 20 minutes.

The atmospheric model used the following numerical levels: 5, 15, 100, 300, 700, 1200, 2000, 3000, 4000, 5000 and 6000 m, while the soil model consisted of the following numerical levels: 0, 5, 10, 15, 20, 25, 30, 40, 50, 75, 100, 150, 200, 250, 300, 400, 600, and 900 cm.

The soil in the simulation was composed of 95% sand, 4% clay, and 1% silt with a surface albedo of 0.2 (adopted from the previous numerical study of Avissar and Mahrer, 1982). Using curves of $\psi(\theta)$ and $K_h(\theta)$ for this type of soil, Hadas (1967) determined the following values for the soil parameters: $\theta_s = 0.4$; $\theta_r = 0.015$; $\lambda = 0.83$; $n = 3.5$; $\psi_{cr} = -0.13$ m; $K_{hs} = 7.0$ m/day.

The meteorological data set obtained from the simulation included the ambient air temperature and specific humidity at 10 m and the wind speed at 5 m, in addition to the incoming solar radiation. Since on the average, cloud coverage is not significant in the study area during the simulated period, its effect on the solar radiation reaching the surface was not considered.

Simulations involved with vegetation

Soil—vegetation model simulations using the refined meteorological data set described in the previous sub-section were performed for the period

specified previously. It was assumed in the current simulations that the horizontal scale of the vegetation domain is relatively small (e.g., not exceeding several hundred meters). This allowed the use of the one-dimensionally derived atmospheric data obtained in the previous sub-section (for a bare soil environment) as also representative of the vegetated slope environment. North and south facing slopes with tilt angles ranging from 0° to 60° (in 7.5° intervals) were considered. The slopes were assumed to be covered entirely with roses (this choice for vegetation resulted from the existing documentation, and associated modeling and experimental studies performed by Avissar and Mahrer, 1982, for this plant). The canopy albedo is actually a function of the slope angle only in hours when the normal radiation at its surface is small (e.g. Kuhn and Suomi (1958); Andre and Viswanadham (1983)). In these hours, however, transpiration is absent or negligible. Therefore, the albedo variations are actually of minor importance in the context of the current study and a typical constant value was adopted. The initial soil volumetric wetness was 10%. Each 24 h of the integration the wetness was adjusted to this level in order to avoid "wilt" of the vegetation for slope situations in which soil moisture is eliminated during the integration period.

The canopy transpiration rates were computed each time step of the simulation (20 min).

RESULTS AND DISCUSSION

The model-predicted monthly amounts of transpiration from the canopy along a south facing and a north facing slope as a function of the slope inclination and the month are given in Fig. 1. For both slopes, there is a general trend of increased transpiration in the summer months, as expected. However, while transpiration rates tend to decrease monotonically for all the months as the north facing slope is steepened, the pattern associated with the south facing slope is more complicated. Along the south facing slope, a general increase of the monthly transpiration rate is computed when the slope is steepened from flat to about 20°—30° for all of the simulated months. When the slope is greater than 30°, however, a reduction of transpiration (which is more emphasized in the summer months compared to the spring and fall months) is predicted.

The solar radiation incoming at the surface is a primary factor in the determination of transpiration from a canopy. It acts directly, through controlling the stomata opening state and indirectly by affecting parameters such as the air and foliage temperature which are involved with transpiration. Therefore, comparing the pattern of global radiation falling on north and south facing slopes will provide preliminary insight into the transpiration pattern differences. We have established a nomogram for the ratio of the incoming global radiation on north facing slopes as compared to that on the equivalent southerly oriented slopes. A formulation for computation of the normal radiation component at the slope surface is given for example in

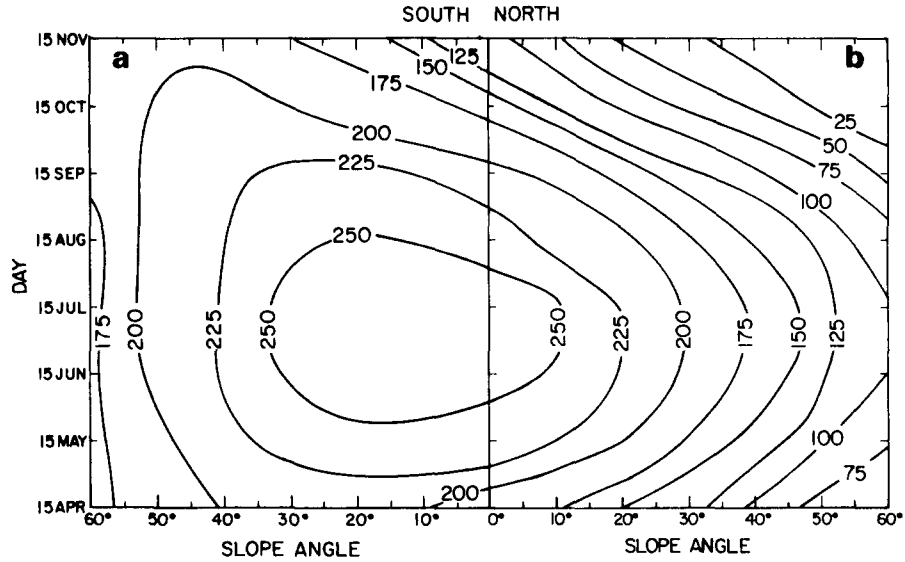

Fig. 1. Monthly transpiration (in mm) from (a) south facing slope vegetation and (b) north facing slope vegetation, as a function of the slope angle and the month.

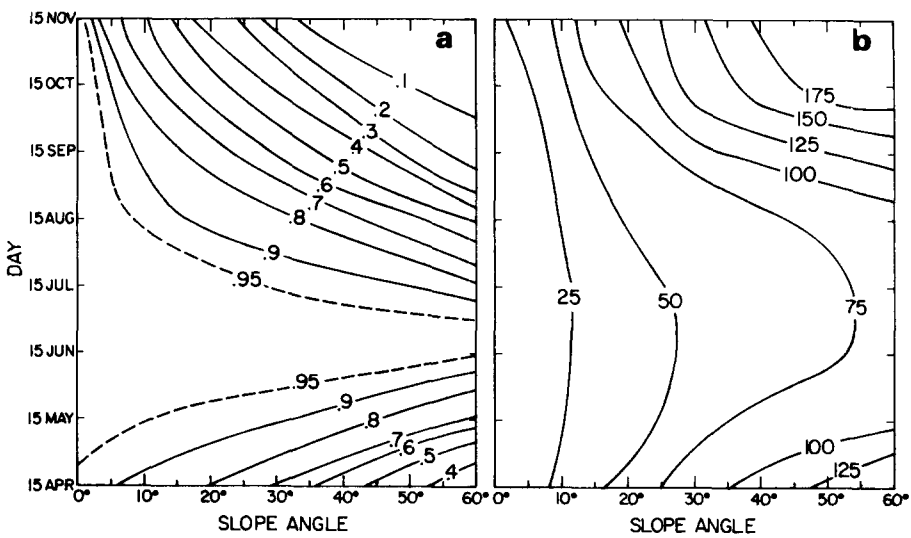

Fig. 2. (a) The ratio of the monthly global solar radiation incoming on north and south facing slopes as a function of the slope angle and the month. (b) The difference in the monthly transpiration (in mm) between north and south facing slopes as a function of the slope angle and the month.

TABLE I

The accumulation of modeled vegetation transpiration along a north facing slope, a south facing slope, and their difference, for the period mid-March to mid-November (in mm)

	Slope angle (°)								
	0	7.5	15	22.5	30	37.5	45	52.5	60
North	1667	1557	1420	1268	1181	924	763	612	468
South	1667	1751	1801	1820	1805	1757	1652	1568	1441
Difference	0	194	381	552	624	833	889	956	973

Bush and Richards (1980). The diffuse radiation was assumed to be 13% of the incoming direct solar radiation. The nonogram in Fig. 2a illustrates this ratio as a function of slope and month of the simulation. During the summer months this ratio is close to unity but generally reduces in the spring and fall months, particularly for steeper slopes. Figure 2b provides a quantitatitive prediction of the differences in transpiration rates between both slopes. This pattern indicates an increase of transpiration with steepening of the slopes and also that the differences are smallest in the summer and largest in the spring and fall. The quantitative evaluation presented in Fig. 2b corresponds with the presentation in Fig. 2a.

The accumulated transpiration for the simulated period is present in Table I. The overall predicted north facing slope transpiration is smaller than the equivalent south facing slope for the simulated period. The accumulated transpiration along the north facing slope decreases monotonically with increasing slope. However, for the south facing slope, an increase of transpiration is predicted when the slope angle increases to 22.5° followed by a decrease for steeper slopes. The transpiration from a south-facing slope of about 45° is similar to that for flat terrain. Therefore, from the point of view of water needs, natural vegetation on south facing slopes in the simulated environment and latitude is likely to prefer very steep slopes.

The results indicate that larger transpiration rates may occur along certain south facing slopes as compared to the north facing slopes during the whole dry season in the subtropics. In general, as the slope steepens, the north–south transpiration difference increases. Hence north facing slopes are likely to provide better environments for the growth of natural shrubs or forests, as is reported in a range of observational studies in subtropical regions. Our study has provided a quantitative evaluation of these situations for a specific case. The results also imply that the irrigation needs for agricultural activity in mountainous areas during the dry season are dependent on orientation and steepness of slopes.

Finally, it would be interesting to adopt this type of modeling approach (however with appropriate modifications in the time scale, area, vegetation type and irrigation patterns) to investigate similarities associated with furrows

which are often used in agricultural activities. In such a study a two-dimensional soil—vegetation model is needed so that the influence of small-scale spatial variations in the surface aspect can be included, at least early in the crop development. In later growth stages, of course, a one-dimensional model may be adequate since the canopy of the agricultural crop in many cases (e.g. cotton) tends to merge. Mahrer (1982), has established such a prototype modeling approach, although it was applied only to a bare soil.

ACKNOWLEDGEMENTS

The current study was supported in part by grant No. ATM-8414181 of the National Science Foundation. Y. Ookouchi was supported by a fellowship from the government of Japan. Acknowledgement is made to the National Center for Atmospheric Research, which is sponsored by the National Science Foundation, for the computing time used in this research. R. Avissar, G. Young and J. Sheaffer provided useful comments on the manuscript. The authors thank Chris Williams, Nancy Duprey, and Bobbie Schwinger for the preparation of the manuscript.

REFERENCES

Andre, R.G.B. and Viswanadham, Y., 1983. Radiation balance of soybeans grown in Brazil. Agric. Meteorol., 30: 157—173.

Atwater, M.A. and Brown, P.S., 1974. Numerical calculation of the latitudinal variation of solar radiation for an atmsophere of varying opacity. J. Appl. Meteorol., 13: 289—297.

Armesto, J.J. and Martinez, J.A., 1978. Relation between vegetation structure and slope aspect in the mediterranean region of Chile. J. Ecol., 66: 881—889.

Atlas of Israel, 1970. Survey of Israel. Ministry of Labour, Jerusalem.

Avissar, R. and Mahrer, Y., 1982. Verification study of a numerical greenhouse microclimate model. Trans. Am. Soc. Agric. Eng., 25: 1711—1720.

Avissar, R., Avissar, P., Mahrer, Y. and Bravdo, B., 1985. A model to simulate plant stomata response to environmental parameters. Agric. For. Meteorol., 34: 21—29.

Businger J.A., Wyngaard, J.C. Izumi, Y., and Bradley, F.F., 1971. Flux—profile relationships in the atmospheric surface layer. J. Atmos. Sci., 28: 181—189.

Bush, G.E. and Richards, M., 1980. Solar geometry and time. In: W.C. Dickinson and P.N. Cheremisinoff (Eds.) Solar Energy Technology Handbook, Part A, Marcel Dekker, New York and Basel, 39—64.

De Vries, D.A., 1963. Thermal properties of soils. In: W.R. Van Wijk (Ed.), Physics of Plant Environment. North-Holland, Amsterdam, 382 pp.

Hadas, A., 1967. Evaporation and drying process in layered soil. Ph.D. Thesis, The Hebrew University, Rehovot, Israel, 161 pp.

Kuhn, P.M. and Suomi, V.E., 1958. Airborne observations of albedo with a beam reflector. J. Meteorol., 15: 172—174.

Mahrer, Y., 1982. A theoretical study of the effect of soil surface shape upon the soil temperature profile. Soil Sci. 134: 381—387.

Mahrer, Y. and Pielke, R.A., 1977. A numerical study of the airflow over irregular terrain. Beit. Phys. Atm., 50: 98—113.

O'Brien, J.J., 1970. A note on the vertical structure of the eddy exchange coefficient in planetary boundary layer. J. Atmos. Sci. , 27: 1213—1215.

Paegle, J., Zdunkowski, W.G., and Welch, R.M., 1976. Implicit differencing of predictive equation of the planetary boundary layer. Mon. Weath. Rev., 104: 1321—1324.

Philip, J.R. and De Vries, D.A., 1957. Moisture movement in porous materials under temperature gradients. Trans. Am. Geophys. Union, 38: 222—232.

Pielke, R.A. and Mahrer, Y., 1975. Technique to represent the heated planetary boundary layer in mesoscale models with coarse vertical resolution. J. Atmos. Sci., 32: 2288—2308.

Sasamori, T., 1972. A linear harmonic analysis of atmospheric motion with radiative dissipation. J. Meteorol. Soc. Jpn., 50: 505—518.

Shaia, J., 1962. Upper air data for Beer-Ya'aqov. Meteorol. Notes, No. 19, Israel Meteorological Service, Bet-Dagan, Israel, 38 pp.

Whittaker, R.H. and Niering, W.A., 1965. Vegetation of the Santa Catalina Mountains, Arizona: A gradient analysis of the south slope. Ecology, 46: 429—452.

Wyllie, M.R.J. and Gardner, G.H.F., 1958. The generalized Kozeney—Carman equation. World Oil, 146: 210—228.

Zemel, Z. and Lomas, J., 1977. Soil temperature regime in Israel as a basis for agricultural planning and activity. Agromet. Rep., 8/77, Israel Meteorological Service, Bet-Dagan, Israel, 16 pp.